Quaternary Science Reviews 146 (2016) 274–287

Contents lists available at ScienceDirect

Quaternary Science Reviews

journal homepage: www.elsevier.com/locate/quascirev

Holocene changes in monsoon precipitation in the Andes of NE Peru based on $\delta^{18}O$ speleothem records

M.G. Bustamante [a, b, *], F.W. Cruz [a, b], M. Vuille [c], J. Apaéstegui [b, d], N. Strikis [a, e], G. Panizo [f], F.V. Novello [a], M. Deininger [g], A. Sifeddine [b, h], H. Cheng [i, j], J.S. Moquet [a], J.L. Guyot [h], R.V. Santos [k], H. Segura [d], R.L. Edwards [j]

[a] Universidade de São Paulo, Instituto de Geociências, Rua do Lago 562, CEP: 05508-080 São Paulo, Brazil
[b] LMI PALEOTRACES (IRD, UPMC, UFF, Uantof, UPCH), Departamento de Geoquímica, Universidade Federal Fluminense, Niteroi, RJ, Brazil
[c] Department of Atmospheric and Environmental Sciences, University at Albany (SUNY), Albany, NY 12222, USA
[d] Instituto Geofísico del Perú, Lima, Peru
[e] Departamento de Geoquímica, Universidade Federal Fluminense, Niteroi, RJ, Brazil
[f] Instituto de Matemática y Ciencias Afines, Universidad Nacional de Ingeniería, Lima, Peru
[g] UCD School of Earth Sciences, Universtiy College Dublin, Belfield, Dublin 4, Ireland
[h] GET, HYBAM (IRD-CNRS-UPS Toulouse), IRD, Lima, Peru
[i] Institute of Global Environmental Change, Xi'an Jiaotong University, Xi'an 710049, China
[j] Department of Earth Sciences, University of Minnesota, Minneapolis, MN 55455, USA
[k] Universidade de Brasília, Instituto de Geociências, Campus Universitário Darcy Ribeiro, CEP: 70910-900 Brasília, Brazil

ARTICLE INFO

Article history:
Received 31 July 2015
Received in revised form
14 May 2016
Accepted 18 May 2016

Keywords:
South American Summer Monsoon
Speleothem
Northeastern Peruvian Andes
Stable isotopes
Paleoclimate
Holocene

ABSTRACT

Two well-dated $\delta^{18}O$-speleothem records from Shatuca cave, situated on the northeastern flank of the Peruvian Andes (1960 m asl) were used to reconstruct high-resolution changes in precipitation during the Holocene in the South American Summer Monsoon region (SASM). The records show that precipitation increased gradually throughout the Holocene in parallel with the austral summer insolation trend modulated by the precession cycle. Additionally the Shatuca speleothem record shows several hydroclimatic changes on both longer- and shorter-term time scales, some of which have not been described in previous paleoclimatic reconstructions from the Andean region. Such climate episodes, marked by negative excursions in the Shatuca $\delta^{18}O$ record were logged at 9.7–9.5, 9.2, 8.4, 8.1, 5.0, 4.1, 3.5, 3.0, 2.5, 2.1 and 1.5 ka b2k, and related to abrupt multi-decadal events in the SASM. Some of these events were likely associated with changes in sea surface temperatures (SST) during Bond events in the North Atlantic region. On longer time scales, the low $\delta^{18}O$ values reported between 5.1-5.0, 3.5–3.0 and 1.5 ka b2k were contemporaneous with periods of increased sediment influx at Lake Pallcacocha in the Andes of Ecuador, suggesting that the late Holocene intensification of the monsoon recorded at Shatuca site may also have affected high altitudes of the equatorial Andes further north. Numerous episodes of low SASM intensity (dry events) were recorded by the Shatuca record during the Holocene, in particular at 10.2, 9.8, 9.3, 6.5, 5.1, 4.9, 2.5 and 2.3 ka b2k, some of them were synchronous with dry periods in previous Andean records.
© 2016 Elsevier Ltd. All rights reserved.

1. Introduction

The South American Summer Monsoon (SASM) variability in Peru during the Holocene has been the focus of many studies (Hansen and Rodbell, 1995; Abbott et al., 1997a,b; Seltzer et al., 2000; Baker et al., 2001; Abbott et al., 2003; Bush et al., 2005; van Breukelen et al., 2008; Reuter et al., 2009; Bird et al., 2011a,b; Cheng et al., 2013a; Kanner et al., 2013; Apaéstegui et al., 2014). However, paleo-hydrological variations in western Amazonia and the northeastern Peruvian Andes are still poorly documented. Understanding how SASM precipitation changed in this region, during the past and the mechanisms controlling this variability, is of major interest because the main tributaries of the Amazon River originate along the eastern flank of the Andean Cordillera. Hence, changes in the SASM behavior over high terrains in the Andes may serve as a

* Corresponding author. Universidade de São Paulo, Instituto de Geociências, Rua do Lago 562, CEP: 05508-080 São Paulo, Brazil.
E-mail address: bustamanterosell@gmail.com (M.G. Bustamante).

http://dx.doi.org/10.1016/j.quascirev.2016.05.023
0277-3791/© 2016 Elsevier Ltd. All rights reserved.

significant contributor to floods or droughts in the lowlands of the western Amazon Basin (Moquet et al., 2011). However, it remains poorly understood and documented how sensitively the SASM has responded along the Andean foothills to extreme climate events, known to have affected other areas of the continent during the Holocene, as seen in central-eastern Brazil (Strikis et al., 2011).

The impact of summer insolation changes on SASM activity in the southern latitudes of the South American tropics and subtropics has been widely documented in several paleoclimatic records from the lowlands (Cruz et al., 2005, 2006; Wang et al., 2006; van Breukelen et al., 2008; Mosblech et al., 2012; Cheng et al., 2013a) to the high Andes (Thompson et al., 2006; Seltzer et al., 2000; Bird et al., 2011a,b; Kanner et al., 2013; Fornace et al., 2014). These records from the northern to central Andes are characterized by a gradual intensification of the SASM throughout the Holocene and they all show an overall opposite trend to those of the northern hemisphere monsoons (Cheng et al., 2012), in response to increasing (decreasing) southern (northern) hemisphere summer insolation related to the precessional cycle. During the early Holocene proxy records suggest that the SASM was very weak, in particular over the northwestern Peruvian Amazon, where speleothem records indicate that the SASM intensity at that time was the weakest ever recorded during the last 250 ka (Cheng et al., 2013a).

Abrupt variability in monsoon precipitation during the last millennium has been documented in Andean paleoclimate records, in periods corresponding to the Medieval Climate Anomaly (MCA) and the Little Ice Age (LIA), which are respectively marked by weaker and stronger SASM activity (Reuter et al., 2009; Bird et al., 2011b; Vuille et al., 2012; Novello et al., 2012; Kanner et al., 2013; Apaéstegui et al., 2014). Other paleorecords from South America (Baker et al., 2005; Strikis et al., 2011; Novello et al., 2012; Moreira-Turcq et al., 2014) have revealed abrupt changes in monsoon precipitation linked to cooler North Atlantic SST during the Holocene Bond events (Bond et al., 2001). However, Andean paleorecords showing abrupt precipitation changes across the whole Holocene period are scarce. One reason for this scarcity may be the lack of well-dated and high-resolution records of sufficient length from the Andean region, most of which are limited to the last two millennia (Vuille et al., 2012). Another possible reason is that the abrupt climatic events that originated over the North Atlantic Ocean possibly had a weaker impact on monsoon precipitation over the Andes during the early and mid Holocene (Carlson et al., 2008), which may have obscured the identification of most Bond events in isotopic records from this region (Thompson et al., 2006; Seltzer et al., 2000; Bird et al., 2011a; Kanner et al., 2013; Fornace et al., 2014).

The Peruvian Andes Cordillera is a barrier between the humid Amazon rainforest to the east and a desert on the Pacific coast (Garreaud et al., 2009). These two sides are affected by distinct climatic systems. The humid Amazon basin is sensitive to changes in the sea surface temperature (SST) of the Atlantic Ocean and in particular to the meridional SST gradients in the tropical Atlantic basin. This Atlantic SST gradient affects the latitudinal displacement of the Intertropical Convergence Zone (ITCZ), which is associated with the SASM activity (Vuille et al., 2012).

The Pacific coast on the other hand is dry due to the cold Humboldt Current and the upwelling of cold waters, which lead to a highly stratified atmospheric column with a stable low-level inversion that prevents convection and moisture influx toward the Andes. This situation is broken up when coastal Pacific SST warms up, as occurs during the warm phase of the El Niño - Southern Oscillation (ENSO) (Garreaud et al., 2009). ENSO influence during the Holocene has been described by studies such as those based on high-altitude lake records from the Ecuadorian Andes, which suggests that El Niño events became progressively more frequent since the mid Holocene (Rodbell et al., 1999; Moy et al., 2002). In addition, it has been suggested that El Niño-like conditions may have contributed to abrupt climate events at millennial time scales over the high Andes of Peru (Kanner et al., 2013). However these summit areas are in the transitional zone between the eastern and western Andean flanks and hence, it remains a challenge to separate the Atlantic from the Pacific SST impact on moisture transport and precipitation over the tropical Andes (Vuille et al., 2000).

To date, most of the isotopic studies performed in Andean regions of Peru are in the relatively dry (puna) central and southern regions (Thompson et al., 2006; Seltzer et al., 2000; Baker et al., 2001, 2005; Bird et al., 2011a,b; Kanner et al., 2013; Fornace et al., 2014) at altitudes at or above 3500 m asl. In the last decade results of some studies from the wetter (rainforests) lowlands (<1000 m asl) near the northeastern Peruvian Andes have been published (van Breukelen et al., 2008; Reuter et al., 2009; Cheng et al., 2013a; Apaéstegui et al., 2014). But so far there are no high-resolution paleoprecipitation studies at mid-altitude Andean locations in-between the high puna regions and the lowland rainforests. Importantly, this narrow transition zone is home to the humid montane forest belt, an extremely relevant biome for biodiversity and biogeography studies, as well as for conservation issues.

In the Andes, this forest zone often spans laterally 10–30 km over the eastern slopes and is located within a narrow temperature range, usually from 1500 m asl (at the elevation where the average minimum temperature drops below 18 °C) to the tree line (around 3500 m asl) (Grubb, 1974, 1977; Young, 1991, 1992; León et al., 1992; Webster, 1995; Young and León, 1999). Within this altitude range, there is a level (typically between 2000 and 3000 m asl) where cloud condensation turns to be more persistent and the cloud forest starts (Grubb and Whitmore, 1966; Grubb, 1977; Bruijnzeel, 2001; Jarvis and Mulligan, 2011). These altitude ranges change depending on the latitude and altitude of the Andean region, and have varied over the last millennia due to climatic and anthropogenic causes, as shown by palynological records from Peruvian montane forests (Hansen and Rodbell, 1995; Bush et al., 2005; Hillyer et al., 2009; Urrego et al., 2010; Valencia et al., 2010). Eventhough, montane forests are diverse and may respond to a climate event in different ways (Gentry, 1988; Bush et al., 2004), little is known about their response to precipitation variability during periods when the SASM changed dramatically.

The complex orographic conditions of the eastern Andes, characterized by high summits, mountain ridges and deep valleys impose sharp boundaries on climate conditions (Guyot, 1993; Ronchail and Gallaire, 2006; Laraque et al., 2007; Espinoza, 2009). This favors the existence of a great diversity of environments and habitats, separated by short distances and renders the flora and fauna of the eastern Andes, especially its endemic species, extremely sensitive to climatic change (Bush et al., 2011). Hence, it is important to have paleoclimate records from the various ecosystems and the different altitude/latitude areas of the Andean region.

In this study, we investigate for the first time a paleo-hydrologic record from a mid-altitude site (1960 m) in the northeastern Peruvian Andes, located in the transition zone between the humid Amazon lowland and the drier highlands. This study is based on two well-dated $\delta^{18}O$-speleothem records from Shatuca cave that record the last 10.5 ka.

2. Study site and modern climatic conditions

Speleothems were collected from Shatuca cave (5.70°S;

77.90°W), located at 1960 m asl in the northeastern Peruvian Andes (Fig. 1), in a Triassic–Jurassic limestone–dolomitic formation (Cobbing et al., 1981). The cave was mapped by the GSBM–ECA team (Fig. S1). It is 670 m long on a south-north axis, and its active and fossil galleries have a total vertical extent of 30 m. Samples used in this study were collected a few meters above the underground river in a distant point from the cave entrance.

Rainfall measurements of the last 5 decades (Peruvian Meteorological Service, SENAMHI, 1964–2014) from different rain gauge stations located near the Shatuca site show a bimodal precipitation regime that is related to the seasonal march of convective precipitation across the region (Fig. 2a). The vast majority of the rainfall (about ~85% of the annual total) occurs between October and April, related to the SASM, while the other 15% is related to residual equatorial rainfall during the winter season.

Along the eastern slopes of the Andes the rainfall amount diminishes with increasing altitude, and areas between ~800 and 900 m asl are wetter (~1600 mm/yr) than regions located between ~1300 and 2500 m asl (~855 mm/yr) (Fig. 2a, c). However, the Andean topography generates a complex rainfall distribution, and depending on the exposure to the moisture being transported from the Amazon, drier and wetter slopes may occur in close proximity (Fig. 2b). TRMM 2B31 satellite data shows that Shatuca cave is in a relatively drier location, when compared to its surroundings, most likely due to orographic effects from mountain ridges further upstream (Bookhagen and Strecker, 2008) (Fig. 2c).

The northeastern Peruvian Andes are directly affected by the northeast trade winds that transport moisture from the tropical North Atlantic to the Amazon. It is at this point that the trade winds veer southeast due to the blocking effect of the Andes and generate a Low Level Jet (LLJ) that transports moisture from the Amazon to the La Plata basin (Paegle, 1998). During the austral wet season this transport is enhanced and the preferential pathway of the LLJ is located more to the west (Poveda et al., 2014). At interannual time scales the last extreme El Niño events (1982–83, 1991–92 and 1997–98) were related to extreme droughts in the northeastern Peruvian Andes (Lavado and Espinoza, 2014), while the strongest floods occurred during the last extreme La Niña events (1970–71, 1973–74, 1975–76, 1988–89) (Marengo and Nobre, 2001; Nogués-Paegle and Mo, 2002; Garreaud et al., 2003, 2009; Grimm, 2011; Lavado and Espinoza, 2014). However, the extreme Amazon droughts of 2005 and 2010 were related to anomalously warm SSTs in the tropical North Atlantic (Marengo et al., 2008, 2012; Espinoza et al., 2011; Lavado et al., 2012).

3. Samples and methods

3.1. Samples

Two speleothems, Sha-2 and Sha-3, collected by the GSBM-ECA team (Bigot, 2008), were used in this study. Sha-2 is a 1.60 m long stalagmite that covers the last 29 ka b2k, with a hiatus between 2.0 and 0.4 ka b2k. In this study we focus on the Holocene period, corresponding to its first 82 cm, which has a mean growth rate of 0.11 mm/yr and a robust chronology based on 19 U/Th dates, yielding an uncertainty (2s) < 1% (Table S1, Fig. S2). In order to fill the depositional gap in Sha-2, we use the Sha-3 sample, a 23.8 cm long stalagmite, formed between 10.5 and 1.3 ka b2k but with a hiatus from 6.3 to 2 ka b2k and a mean growth rate of 0.05 mm/yr. Its chronology is based on 11 U/Th dates, yielding an uncertainty (2s) < 1% (Table S2, Fig. S2). The isotopic profile of Sha-2 is based on 1564 $\delta^{18}O$ samples for the Holocene, which provides a mean resolution of 5 yrs while Sha-3 profile consists of 632 $\delta^{18}O$ samples, with a mean resolution of 7.25 yrs (Fig. S3).

Together both stalagmites (Sha-2 and Sha-3) cover most of the Holocene, with a hiatus between 1.3 and 0.4 ka b2k. The Shatuca composite has an average resolution of ~5.3 years and is composed of 1770 $\delta^{18}O$ isotopic values. To obtain an age for each sample, the isotopic values were linearly interpolated between the U/Th ages.

3.2. Geochronological and isotopic methods

The U/Th geochronology of the stalagmites was determined at the University of Minnesota using an inductively coupled plasma-mass spectrometry (ICP-MS) technique following the procedures described by Cheng et al. (2013b). The b2k notation refers to the age before present, taking the present as 2000 AD, following Rasmussen et al. (2014).

Oxygen isotope ratios are reported as $\delta^{18}O$ relative to the Vienna-*Peedee Belemnite standard* (V-PDB). Thus, $\delta^{18}O = [(({}^{18}O/{}^{16}O)\ \text{sample}/({}^{18}O/{}^{16}O)\ \text{V-PDB}) - 1] \times 1000$. For each measurement, approximately 200 μg of powder were drilled from the sample and analyzed with an on-line, automated, carbonate preparation system linked to a Thermo - Finnigan Delta Plus Advantage mass spectrometer at the Stable Isotope Laboratory of Geosciences Institute of São Paulo University, Brazil (LIESP-CPGeo). The speleothem reproducibility of standard materials is 0.15‰ for $\delta^{18}O$.

Water samples for isotope analyses (8 ml bottles) were collected twice a month between June 2012 and June 2014 in order to evaluate the isotopic signature of precipitation in the isotope rainfall collector installed close to the Palestina cave, located at 870 m asl and 66 km apart from Shatuca cave (Apaéstegui et al., 2014). Water analyses were performed in the Laboratório de Estudos Geodinâmicos e Ambientais at the University of Brasilia (UnB) using a Picarro L2120-i water isotope analyzer, which allows measurements at an analytical precision of 0.1‰ and reports ^{18}O‰ relative to Vienna Standard Mean Ocean Water (SMOW) standard.

3.3. Statistical methods

To better compare records at millennial time scales, some of the figures show the detrended time series, which were obtained by calculating the quadratic polynomial function for the $\delta^{18}O$ curve. This effectively removes the orbital-component of the $\delta^{18}O$ time series, allowing a comparison of the residual time series in the Shatuca record.

In order to evaluate whether the $\delta^{18}O$ signature shows a regionally coherent behavior between Shatuca and previous paleorecords from the SASM region, we use similarity estimators to assess the synchronicity, at a certain lead/lag, between Shatuca composite and each of the other records. To apply these tests, the records were previously detrended and cut to the overlapping period between 10.5 and 1.3 ka b2k.

The similarity estimators, gXCF, gMI and ESF (Rehfeld and Kurths, 2014), are available at the NESTOOLBOX (tocsy.pik-postdam.de/nest.php). To apply these estimators, age modeling was performed on each record using the COPRA algorithm with 1000 Monte Carlo (MC) realizations (Breitenbach et al., 2012) and considering a PCHIP (Piecewise Cubic Hermite Interpolating Polynomial) interpolation (Fritsh and Carlson, 1980).

Each of the MC simulations was compared between records using the similarity estimators. The 1000 values obtained for each estimator were then averaged to find a single result. This procedure is repeated with different time lags for each couple of records being compared. The lag was always applied to the Shatuca record. Hence, when the maximum synchronicity occurs at a positive lag it means that the events were recorded first at Shatuca site.

The Gaussian-Kernel-based cross correlation (gXCF, Rehfeld et al., 2011) is a correlation measure between two time series, calculated with a Gaussian weight factor to account for the

temporal uncertainty of the records. The Gaussian-Kernel-based mutual information (gMI, Rehfeld et al., 2013) is a measure of the dependence (linear or nonlinear) between two random variables (X and Y). It measures the reduction of the uncertainty in the X values, given that Y is known. Here, the letter "g" also refers to a Gaussian weight as in the case of gXCF.

We also use the Event Synchronization Function (ESF, Rehfeld and Kurths, 2014), which is based on the similarity measure of Quian Quiroga et al. (2002). This is a nonlinear correlation measure that evaluates whether the extreme events of a time series, are at a certain temporal distance (calculated according to Rehfeld and Kurths, 2014) or less of the extreme events of the other time series. The original algorithm does not distinguish wet events from dry events, here we implemented a modification to synchronize only the same type of events. Hence, wet (dry) events in Shatuca record will only find a match if a wet (dry) event occurs in the comparing record.

Additionally we use another event synchronization procedure based on Quian Quiroga et al. (2002) Event Synchronization (ES) measure, but modified to take into account the age error bar of each extreme event. This modification consists on calculating an age error bar for each $\delta^{18}O$ for this we use the following simple linear interpolation procedure: for a given data point, at age "t", we identify the neighboring U/Th, t_o and t_r (corresponding to the oldest and most recent of both) with their corresponding age error bars e_o and e_r. Then, the age error bar for the given $\delta^{18}O$ value, e_t, equals:

$$e\_t = e\_o + (e\_r - e\_o)^*(t - t\_o)/(t\_r - t\_o).$$

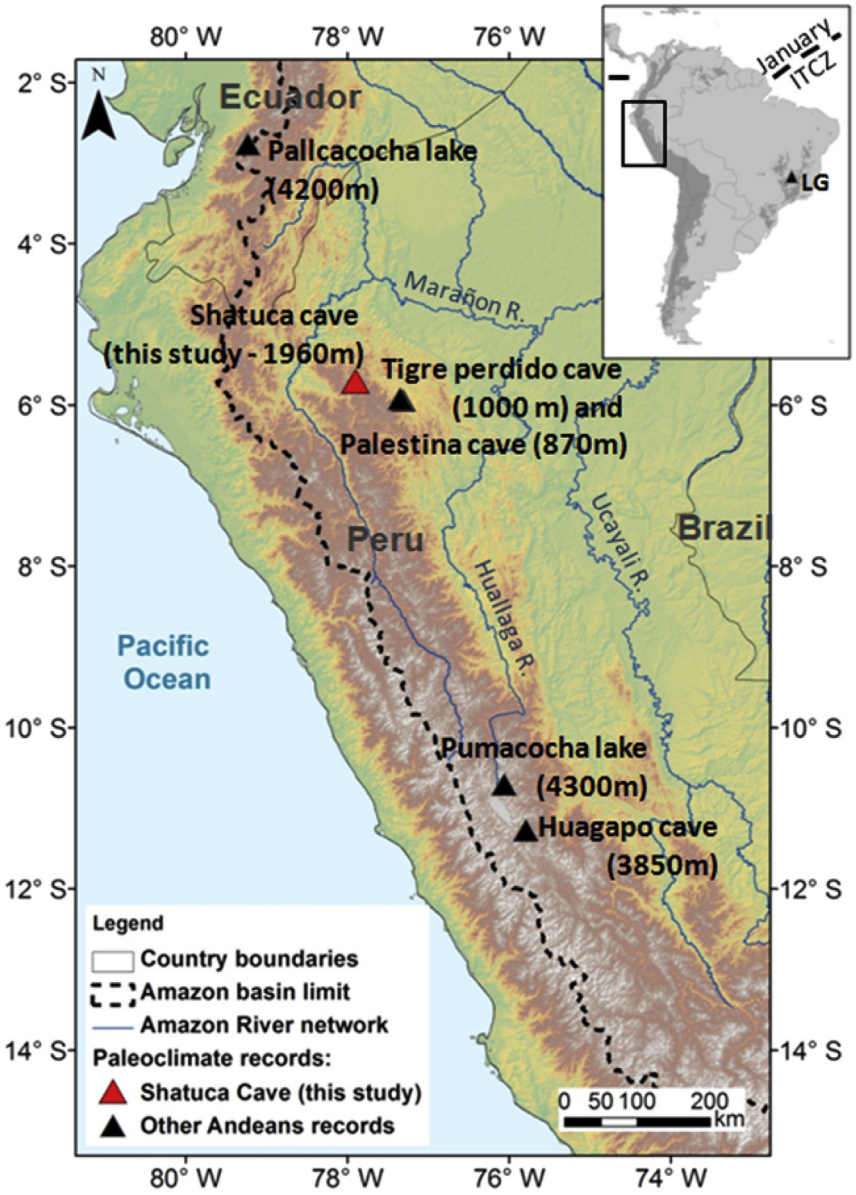

Fig. 1. Location of Shatuca cave record (5.70°S, 77.90°W) (red triangle) and other Andean paleoclimate records (black triangles) used for comparison. These paleoclimate records are Pallcacocha lake (Rodbell et al., 1999; Moy et al., 2002) in southwestern Ecuador; Tigre Perdido cave (van Breukelen et al., 2008) and Palestina cave (Apaéstegui et al., 2014), in the northeastern Peruvian Andes); Pumacocha lake (Bird et al., 2011a,b) and Huagapo cave (Kanner et al., 2013), in the central Peruvian Andes. On the top: Location of Lapa Grande cave record ("LG", black triangle, Strikis et al., 2011) and of the Intertropical Convergence Zone (ITCZ). (For interpretation of the references to colour in this figure legend, the reader is referred to the web version of this article.)

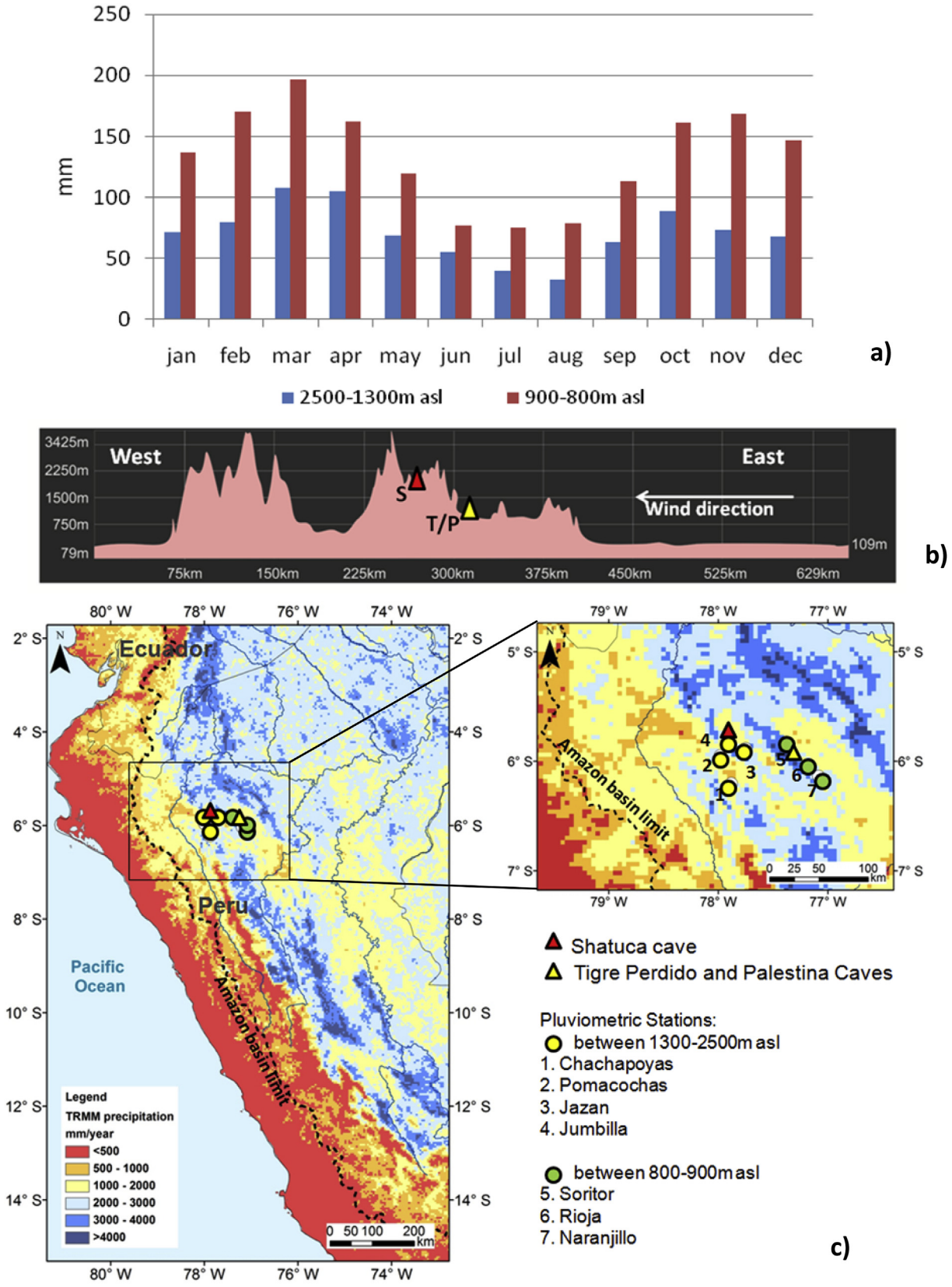

Fig. 2. a) Histogram indicating mean monthly precipitation (1964–2014) in meteorological stations located at mid altitudes (1300–2500 m asl) and lowlands (800-900 m asl). b) Altitude profile, and location of Shatuca "S", Tigre Perdido "T" and Palestina "P"caves. c) Mean annual precipitation from TRMM 2B31 satellite data (average from 1998 to 2009, in mm/yr). Shatuca (Tigre Perdido and Palestina) cave location is indicated with a red (yellow) triangle and pluviometric stations are indicated with circles. Meteorological stations located at the drier mid altitudes, as Shatuca cave, are represented by yellow circles (1–4) and those located at the wetter lowlands, as Tigre Perdido and Palestina caves, by green circles (5–7). (For interpretation of the references to colour in this figure legend, the reader is referred to the web version of this article.)

Then a local tolerance, LT, to identify synchronizations between wet events in both time series is calculated using the age error bars, e_1 and e_2, of the extreme events being compared in each time series: LT = (e_1 + e_2). A similar procedure is used to identify event synchronization between the extreme dry events in both time series. These extreme events were identified using a ±2 sigma range.

In addition, to find the dominant periodicities at which the Shatuca $\delta^{18}O$ record varies over the course of the Holocene, spectral analysis (REDFIT) (Shulz and Mudelsee, 2002) and wavelet analysis techniques (Torrence and Compo, 1998) were performed with the software PAST (Hammer et al., 2001). For the REDFIT analysis, the data was fitted by an AR(1) model with the original linear interpolations between U/Th dates of the record, using the runs parameters: window = rectangle, oversample = 1 and segments = 1. For the wavelet analysis the time series was equally-spaced interpolated to 5 years using a lag of 0.5 years and p-values of 0.05.

4. Basis for interpretation of $\delta^{18}O$ values

The oxygen isotopic composition of precipitation over tropical South America is principally controlled by Raleigh-type fractionation during rainout and is not simply a measure of precipitation amount at the site (Vuille et al., 2003; Vuille and Werner, 2005; Vimeux et al., 2005; Schmidt et al., 2007). Other factors such as moisture source area, condensation temperature and degree of rainout upstream might also exert a significant influence on the isotopic signature of rainwater and therefore on the $\delta^{18}O$ variation of speleothems. In order to address this question, the results of a monitoring program for rainwater isotopic composition in the Palestina cave area are presented (Apaéstegui et al., 2014) (Fig. S4). Precipitation seasonality is similar at this site with most of the annual rainfall related to SASM activity, from October to April (Fig. 2a). During the monitored period a progressive increase (decrease) in the $\delta^{18}O$ values is observed during the dry (monsoon) season. However, the relationship between $\delta^{18}O$ and rainfall amount is not evident on sub-monthly time scales and is statistically weak ($r^2 = 0.07$; $p < 0.01$). In particular, the lowest $\delta^{18}O$ value observed in early November/2012 does not coincide with the rainiest period in the time series. On the other hand our data show that the $\delta^{18}O$ values of rainfall increase rapidly by approximately 7‰ from the mid-June 2012 to August 2012. Then the $\delta^{18}O$ values became substantially depleted from mid-October 2012 to the end of the first monsoon season (April 2013) with $\delta^{18}O$ values decreasing by up to 6‰. It takes approximately one month after the demise of the monsoon season for the $\delta^{18}O$ values to start increasing again, reaching the highest values from August to September 2013 as observed in the previous season (Fig. S4). The isotopic composition of rainfall is still very negative two to three weeks after a substantial decline in rainfall because the remaining vapor is much depleted in ^{18}O such as observed in May/13 and May/14. The opposite is also valid for the response of $\delta^{18}O$ to intra-seasonal breaks in precipitation, for instance the relatively low values of $\delta^{18}O$ seen in mid January/2013 to mid February/2013 and also in early December/2013 and early March/2014.

Although the most depleted $\delta^{18}O$ values are observed during the rainiest months of the monsoon season, it is apparent that the rainfall isotopic signature is significantly influenced by distal processes associated with the long-range transport of moisture from the tropical Atlantic across the Amazon Basin towards the tropical Andes (Garcia et al., 1998; Salati et al., 1979; Vimeux et al., 2005; Vuille et al., 2003). Because of rainout upstream along the moisture trajectory, the residual water vapor becomes progressively more depleted in ^{18}O of precipitation over the course of the monsoon season. Our data is consistent with results from ECHAM4 model simulations of $\delta^{18}O$ in monsoon rainfall in South America where a stronger SASM is associated with more depleted values in ^{18}O of summer precipitation (Vuille and Werner, 2005) and also with recent measurements of snowfall $\delta^{18}O$ in the Andes of Peru, showing a similar progressive depletion of $\delta^{18}O$ over the course of the monsoon season (Hurley et al., 2015).

The removal of moisture from an air mass is temperature-dependent. Vapor condensation requires cooling of the air mass and because of Rayleigh distillation implies a process of equilibrium fractionation (Dansgaard, 1964; Lachniet, 2009). In this case, the $\delta^{18}O$ of the condensed moisture from a saturated air mass becomes more negative with lower temperature (Dansgaard, 1964). A typical range for the altitude effect is −1.9‰ $\delta^{18}O$ km^{-1}, related to the mean annual temperature decrease with height along the local environmental lapse rate that is typically −5 to −6 °C km^{-1} (Gonfiantini et al., 2001). On the other hand, the cooling of an air parcel, because of orographic lifting in the Andes, is unlikely to be a major factor explaining $\delta^{18}O$ variations in rainwater feeding cave speleothems. Nevertheless, this difference in the $\delta^{18}O$ from low to high Andes might be influenced by average temperature inside the caves, significantly cooler in Shatuca cave (~18 °C) than in Tigre Perdido (~22 °C) or by significantly lower precipitation at the Shatuca site, being only about half the amount of the lowland site.

However, the high amplitude of $\delta^{18}O$ values observed in Shatuca cannot be accounted for the temperature dependence of isotope fractionation between calcite and drip water in the cave. For instance, a decrease of more than 3‰ observed during the Holocene in the speleothems would require an increase in cave temperature of about 12 °C by considering the temperature-dependent fractionation between calcite and water of −0.24‰ per °C (Friedman and O'Neil, 1977). This temperature range is inconsistent with changes in mean annual air temperature outside the cave, which did not amount to more than a few degrees over this period at the most (van Breukelen et al., 2008).

While discussing the Shatuca isotopic signature, we will consider that more negative $\delta^{18}O$ values in the studied speleothems most likely reflect an intensification of the SASM, associated with enhanced rainout upstream across the Amazon Basin (Vuille and Werner, 2005). Higher $\delta^{18}O$ values in speleothems, on the other hand, are likely related to periods of a weaker SASM, when rainfall is more influenced by recycled moisture within the basin. It is of course possible that periods of SASM intensification also lead to increased precipitation in-situ over the Andes and that periods of weaker SASM might have seen decreased rainfall as is observed today. But since the region is also influenced by isotopically heavier residual equatorial rainfall, changes in absolute local precipitation amounts cannot be precisely constrained from our speleothem oxygen isotope records.

5. Results and discussion

5.1. Statistical tests

A thousand Monte Carlo Simulations were made for Shatuca composite age model, shown in Figure S5a, and for each of the records used for comparison (results not shown). The gMI shows similar results for all comparisons, while the gXCF shows values between −0.15 and 0.15. Since the main interest is related to recognize the synchronization of extreme events recorded in the Shatuca $\delta^{18}O$ time series with other paleorecords from South America, the discussion is based on the results given by the ESF test which allows to estimate event synchronization at different lags between the time series (Figure S5b).

In the comparison with lowland records (Tigre Perdido and Lapa Grande), the ESF presents a significant synchronization with Lapa

Grande (0.26) if a lag of −50yrs is applied to Shatuca record. Similarly, if the lag applied is of +40yrs, there is also high synchronicity with the events that occurred in both lowland records, Tigre Perdido (0.22) and Lapa Grande (0.14), respectively.

In the comparison with highland records (Huagapo and Pumacocha records), a peak in ESF is observed in the comparison with Huagapo (0.27) if a lag of −100yrs is applied to Shatuca record, similar high values (0.27) are observed if the lag applied goes from −50 to 10 yrs. The case of Pumacocha is different, considering lags that go from −20 to 200 yrs, the synchronization increases monotonically from 0.2 to 0.3. This is due to the high chronological error in Shatuca and Pumacocha records during the late Holocene, given that synchronizations found during the early and mid Holocene occurred at lags around −50yrs (results not shown).

Note that in Fig. S5c, the comparison with the Pumacocha record which shares only three synchronous events with Shatuca record however, high ESF values (0.2) were obtained at a 0yrs lag for this comparison in Fig. S5b. This is in part due the high resolution of Pumacocha and Shatuca during the late Holocene, which generates high ESF values due to the number of synchronizations. The opposite occurs with Tigre Perdido record, that shares seven synchronous events with Shatuca record (Fig. S5c) but due to the low resolution of the lowland record the ESF shows values around 0.1 (Fig. S5b).

These results reveal statistical confidence on event synchronization for the SASM region and indicate that the $\delta^{18}O$ signature shows a regionally coherent behavior. Note that throughout the Holocene the strongest event synchronicity was found with the Lapa Grande record (lag applied to Shatuca of −50yrs), which has been interpreted as a recorder of Bond events in South America (Strikis et al., 2011) (Fig. S5b,c), suggesting that the isotopic events in Shatuca record are related to large scale events within the SAMS region.

The wavelet analysis (Fig. S6d) of the detrended isotope record of Shatuca indicates strong centennial periodicities between 300 and 700 yrs throughout the intervals ~9.2–8.2 and ~7.0–2.0 ka b2k. In addition, the spectral analysis (Fig. S6a) suggests that this range of periodicities has a main periodicity centered at ~445 yrs. Abrupt events occurring at the intervals 10.0–7.8 and ~7–1.8 ka b2k (Fig. S6d) are probably associated with the 102 and 137 yrs periodicities, highlighted by the spectral analysis in Fig. S6b. However, the 175 yrs periodicity (Fig. S6b) is probably an analytical artifact due to $\delta^{18}O$ data interpolations of the Sha-2 and Sha-3 stalagmites around 6 ka b2k (Fig. S6d).

5.2. Long-term changes driven by summer insolation

Following the early (10.5–8.2 ka b2k), mid (8.2–4.2 ka b2k) and late (4.2–0 ka b2k) Holocene definition of Walker et al. (2012), it is possible to observe that the $\delta^{18}O$ signal decreases from −3.4‰ to −7.3‰ during the transition from the early to the late Holocene (Fig. 3). Indeed the long-term decreasing trend in the Shatuca isotopic record appears to follow austral summer insolation for February at 5°S (Laskar et al., 2004), where lower (higher) values of insolation (W/m^2) are contemporaneous with less (more) depleted $\delta^{18}O$ values in the Shatuca record during the early (late) Holocene. Previous isotopic paleorecords from the tropical Peruvian Andes (Seltzer et al., 2000; van Breukelen et al., 2008; Bird et al., 2011a; Kanner et al., 2013) show similar trends for the Holocene and have been interpreted as showing an enhancement of the SASM precipitation in response to increasing austral summer insolation during the Holocene. This trend seen in the tropical Andes is also reported by speleothems at cave sites influenced by the SASM in subtropical Brazil (Cruz et al., 2005, 2006; Wang et al., 2006). This similarity suggests that the gradual summer insolation increase in the southern hemisphere also affected the Shatuca site during the Holocene.

In Fig. 3, the comparison between Shatuca and other northeastern and central Peruvian Andean records confirms that the most enriched ^{18}O-values occurred during the early Holocene, likely because of a weakened monsoon and hence diminished convective activity over the SASM region and less depleted moisture arriving to the Andes. However, this is not consistent with central Amazonian records (e.g. Mayle and Power, 2008; Cordeiro et al., 2008, 2014), in which the driest period is the mid Holocene. This suggests that precipitation over the western Amazon basin may have been more strongly influenced by austral summer insolation than other areas of the Amazon during the Holocene. Moreover, after the gradual decrease of the isotopic signal from 10.5 to ~3.5 ka b2k, related to the increasing austral summer insolation, the decreasing trend flattens out over the most recent 2.5 ka b2k; a change also seen in other Andean records (Bird et al., 2011b).

5.3. Abrupt changes in SASM rainfall

The long-term negative trend in $\delta^{18}O$ at Shatuca is accompanied by multiple abrupt changes (>1‰ in less than 100 yrs) superimposed on the gradual $\delta^{18}O$ decrease (Fig. 4). Changes toward wetter conditions occurred successively at 9.7–9.5, 9.2, 8.4, 8.1, 5.0, 4.1, 3.5, 3.0, 2.5, 2.1 and 1.5 ka b2k, some of them are likely related to the Bond events in the North Atlantic region. In addition abrupt variations toward drier conditions, not previously reported, occurred at 10.2, 9.8, 9.3, 6.5, 5.1, 4.9, 2.5 and 2.3 ka b2k, where those logged at 2.5 and 2.3 ka b2k seem to point the end of the gradual trend toward wetter conditions imposed by insolation.

Except for the last millennium (Reuter et al., 2009; Bird et al., 2011b; Vuille et al., 2012; Apaéstegui et al., 2014), no abrupt events or rapid state changes in monsoon intensity have been discussed in detail in Andean Holocene records (Bird et al., 2011b; Kanner et al., 2013). Hence the abrupt changes toward high/low $\delta^{18}O$ values, characterize Shatuca as the Andean record with the highest variability in the early and mid Holocene (Fig. 4). These abrupt shifts become more visible in the detrended $\delta^{18}O$ time series (Fig. 4).

The next sections will describe in detail the centennial- to decadal-scale variability recorded in Shatuca and other Andean records during the Holocene, in order to determine if the $\delta^{18}O$ time series have a regional signature, some of them potentially related to Bond events.

5.3.1. Early Holocene (10.5–8.2 ka b2k)

Previous lake, pollen, ice-core and cave paleorecord studies usually point to the dryness of the early Holocene but the presence of wet events is not so evident. For this period, the Shatuca record shows shifts of a larger magnitude during the early Holocene than any other isotope record from the Andean region. Abrupt drops toward lighter $\delta^{18}O$ values, characterized by magnitude shifts of about 1.5–2.0‰, occurred in Shatuca around 9.7–9.5 and 8.2–8.0 ka b2k (Fig. 4). Other wet periods, although not abrupt, occurred at 9.2 and 8.4 ka b2k. None of the four events were reported in previous stable isotope studies performed in the Andes.

The first wet period recorded at Shatuca is a two-phased wet event, marked by abrupt $\delta^{18}O$ decreases of ~1.5 and ~2.0‰ at 9.7 and 9.5 ka b2k, respectively. Although, not clearly recorded in other Andean records such as Tigre Perdido cave or Lake Pumacocha (Fig. 4), it seems to be related to Bond event 6.

The events logged at 9.2 and 8.4 ka b2k in Shatuca were simultaneous with two wet events logged at 9.3 and 8.3–8.2 ka b2k in the Lapa Grande cave record (Fig. S5c). Furthermore, a drop in $\delta^{18}O$ of about 1.5‰ is observed at 8.1 ka b2k in Shatuca coinciding

with the timing of the second phase of the 8.2 ka b2k event (Cheng et al., 2009). Fig. S7 shows that this event was clearly recorded as a two-phased event (8.2 and 8.1 ka b2k) by the Tigre Perdido cave record (van Breukelen et al., 2008). Note that the only synchronization for wet events in Shatuca with other Andean record by the ES method (Fig. S5c) was found during the early Holocene with Tigre Perdido, this event is the one related to the 8.2 ka b2k. The low and mid altitudes of the northeastern Andes, probably due to its location, seem to be a region where the 8.2 ka b2k event can be recorded by high resolution paleorecords (Fig. S5c, S7).

On the other hand, the occurrence of these events is not observed at highland sites such as Lake Pumacocha, where the amplitude changes were almost negligible. It is possible that given the low intensity of summer insolation during the early Holocene, moisture transport during Bond events was not sufficient to sustain a vigorous monsoon circulation in the high Andes, where Lakes Pumacocha (Bird et al., 2011a, Fig. 4) and Pallcacocha (Moy et al., 2002, Fig. 5) are located, thereby only affecting climate at low and mid-altitudes. However, the identification of climatic changes at multidecadal time scales in Lake Pumacocha may also be somewhat hampered by the larger chronologic uncertainty (200 yrs) combined with the lower isotopic resolution of the record at this time period (Bird et al., 2011a).

Finally, three extremely dry periods (10.2, 9.8 and 9.3 ka b2k) were also recorded by Shatuca record at the beginning of the early Holocene. The latter was abrupt and also recorded by the Tigre Perdido record (Fig. S5c, S7). Again none of these extreme dry events were recorded in the high altitude record of Pumacocha lake, probably due to its lower temporal resolution and large chronologic uncertainty.

5.3.2. Mid Holocene (8.2-4.2 ka b2k)

Different from the early Holocene, multi-decadal events impacting monsoon rainfall on a regional scale were more evident in Andean records during the mid Holocene. These changes were synchronous between Shatuca, Huagapo (Kanner et al., 2013) and Lapa Grande (Strikis et al., 2011) cave records.

When the insolation influence is removed from these records, the synchronicity between these $\delta^{18}O$ SASM records is apparent not only during the most intense monsoon periods but also during relatively weak monsoon phases (Fig. 4). For example, Shatuca record exhibits abrupt precipitation changes toward drier monsoon periods at 6.5, 5.1 and 4.9 ka b2k that were also recorded by other South American records (Fig. S5c, S8), not necessarily as abrupt changes, but as anomalous periods characterized by decreased humidity during the monsoon season, interrupting the long-term trend toward more intense SAMS driven by higher austral summer insolation (Fig. 3). Previous studies have already identified the occurrence of dry events during the mid Holocene (e.g. Hansen and Rodbell, 1995; Bush et al., 2005; Mayle and Power, 2008; Hillyer et al., 2009; Urrego et al., 2010; Valencia et al., 2010; Stansell et al., 2013). However, no clear timing was defined for these events due to insufficient temporal resolution and lack of robust geochronological control.

Although the dry event at 6.5 ka b2k was never specifically mentioned in any other oxygen isotope records from the Andes, it is also evident in the Huagapo record indicating that, within age errors, it affected at about the same time both the northeastern and the central Peruvian Andes (Fig. S5c, S8). In addition, it can also be identified in the Lapa Grande monsoon record, located in eastern Brazil (Strikis et al., 2011), which suggests a widespread impact of this event (Fig. S5c).

After an increase in $\delta^{18}O$ values from 5.2 to 5.1 ka b2k (also recorded by Huagapo record as a extreme dry event), an abrupt shift to lower $\delta^{18}O$ values occurred at Shatuca time series, marking the start of a series of abrupt decadal-scale events that prevailed from 5.06 to 4.96 ka b2k. To verify the structure of this series of events, the portion between the U/Th dates 5182 ± 29 and 4830 ± 53 yr, was sampled at a higher resolution (2 years), revealing the occurrence of four abrupt changes of similar amplitude. Henceforth we will refer to this period characterized by abrupt events as the “5 ka b2k event”.

This event recorded in the northeastern Andes was synchronous with the occurrence of Bond event 4 in the Atlantic Ocean, the strongest of Bond events (Bond et al., 2001), and with a series of wet events recorded between 5.1 and 4.8 ka b2k at Lapa Grande (Strikis et al., 2011), that mirrors the abruptness of the Shatuca 5 ka b2k event, albeit on slightly longer time scales (Fig. 4). The 5 ka b2k event is also evident in the Pumacocha lake record (Bird et al., 2011a) as a period of changes which shows abrupt shifts to negative $\delta^{18}O$ values between 4.91 and 4.87 ka b2k, and in the Huagapo cave record (Kanner et al., 2013), as a change toward lower isotopic values between 5.04 and 4.95 ka b2k.

The 5 ka b2k event that lasted ~100 years in the Shatuca and Huagapo records, and only ~40 years in the Pumacocha lake record, lasts significantly longer in Lapa Grande (~300 years). One reason which might explain why the Lapa Grande record shows a much longer 5 ka b2k event, may be that the slow deposition rate during this time period may have affected the sampling. Hence, Shatuca record suggests that the 5 ka b2k event was a period of drastic changes in precipitation, apparently composed by 4 abrupt changes in precipitation that occurred over a period of approximately 100 years.

In addition, an approximately 100 yr long dry period followed this 5 ka b2k event at Shatuca, which was also present in the Huagapo and Pumacocha records, although not as an extreme dry event. Nonetheless this suggests that the 5 ka b2k event took place in-between two relatively long dry periods that were felt in the northern and central Peruvian Andes, at both mid- and high altitudes (Fig. S8).

Previously this 5 ka b2k event structure was not discussed in any detail for the Andean region, but some paleorecords already indicated that an abrupt change toward cooler (Thompson et al., 2006) and/or wetter conditions (Buffen et al., 2009; Stansell et al., 2013) occurred. In fact, several records around the globe have recorded a climatic change between 5.5 and 5.0 ka b2k (Buffen et al., 2009). However, while some studies suggest that an event at ~5.2 ka b2k was part of an abrupt widespread climatic change (Magny and Haas, 2004) others suggest a more gradual change (Fleitmann et al., 2003). The abruptness of the 5 ka b2k event remains a topic of active discussion (Claussen, 2008), although Shatuca record and previous isotopic paleorecords used for comparison in this study would clearly suggest that the event was in fact characterized by a series of abrupt events.

5.3.3. Late Holocene (4.2-0 ka b2k)

Recognizing relatively abrupt climate events during the last 4.2 ka b2k is more difficult in the Shatuca isotope record because the U/Th chronology is not that precise, due to high content of detritic Th in the Sha-2 speleothem in the late Holocene. However, the ESF and ES obtained results for this period and our comparison of isotope records from different regions in South America, suggest that some events of enhanced SASM intensity, not previously discussed in similar studies performed in the Andes, occurred in a large area over the continent (Fig. S5b,c).

For instance, multidecadal $\delta^{18}O$ wet excursions in our Shatuca record, varying around 1.0–2.0‰ in amplitude, occurred at about 4.1, 3.5, 3.0, 2.5, 2.1 and 1.5 ka b2k and had similar counterparts, within age uncertainty, during wet monsoon periods recorded in Tigre Perdido at 4.0, 3.4, 3.0, 2.5 and 2.0 ka b2k (Fig. S5c, S9). The

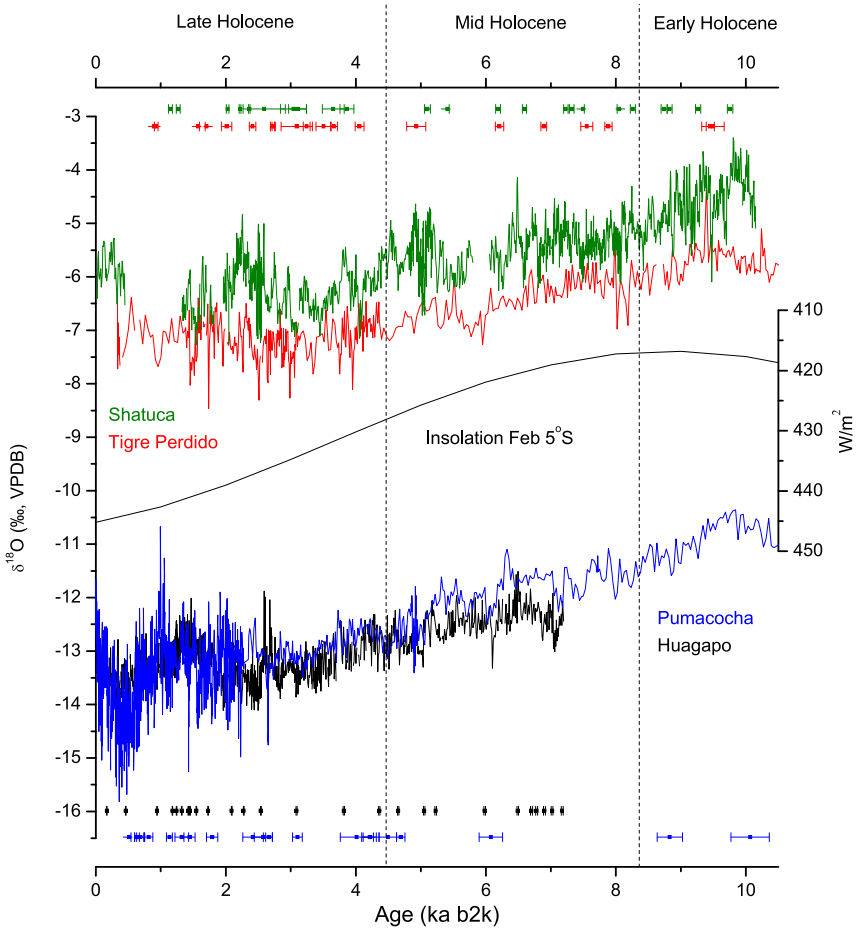

Fig. 3. Comparison between isotope records from the central and northeastern Peruvian Andes and the insolation trend (black line) for the month of February at 5°S (Laskar et al., 2004). Shatuca cave (1960 m asl) record in green (this study) and Tigre Perdido cave (1000 m asl) record in red (van Breukelen et al., 2008) are located at lower altitude sites in the northeastern Peruvian Andes, while the Pumacocha (4300 masl) lake record in blue (Bird et al., 2011a) and the Huagapo cave (3850 m asl) record in black (Kanner et al., 2013) are situated in high mountain areas of the central Peruvian Andes. Early, Mid and Late Holocene subdivision according to Walker et al. (2012). Ages and error bar for each record are also shown. (For interpretation of the references to colour in this figure legend, the reader is referred to the web version of this article.)

event logged at 4.1 ka b2k was possibly related to Bond event 3, indicating that this Bond event affected low- and mid-elevations of the northeastern Andes, but not the high-altitude regions (Fig. S5c).

Few of these climate anomalies, are evident in the central Andes and the Brazilian lowlands. For instance, at Huagapo and Lapa Grande caves, only the 3.0, 2.5 and 2.0 ka b2k wet events are observed, while in the Pumacocha lake record only the 2.5 and 2.0 ka b2k wet events were recorded (Fig. S9). Within age uncertainties, the wet events logged at 3.5 and 3.0 ka b2k in the Shatuca record could be related to Bond event 2 (Bond et al., 2001). However, it remains more complicated to define whether the events logged around 2.5 and 2.0 ka b2k in all Andean records, were related to a global event such as Bond event 2, or to a regional Andean event (Fig. S5c, S9). The wet event logged at 1.5 ka b2k in the Shatuca record was not an extreme wet event in any other Andean record; however, it seems to be related to Bond event 1 and to negative isotopic incursions recorded by the Tigre Perdido and Pumacocha isotopic time series.

On the other hand, the Shatuca record shows that around 2.5 ka b2k dry and wet extreme events occurred (Fig. S9). The dry events at 2.5 ka b2k seem to be related to the dry peaks that occurred in Huagapo at 2.6 ka b2k and given the larger chronological error in Shatuca record at this time period, these dry peaks in Shatuca record appear to be also related to a dry event in Tigre Perdido $\delta^{18}O$ time series logged at 2.3 ka b2k (Fig. S5c, S9). In addition, a long dry period that lasted more than 200 years and culminated in the most enriched $\delta^{18}O$ values of the late Holocene in the Shatuca record is logged at about 2.3 ka b2k, synchronous with the dry event in the Tigre Perdido record (Fig. S5c, S9).

In general, during the late Holocene several event synchronicities were found between northeastern records, and some with high altitude central Andean records (Fig. S5c, S9). It is interesting to note that the dry events logged at 2.5 and 2.3 ka b2k apparently marked the end of the long-term insolation influence on the Andean records at different altitudes (Fig. 3).

In general, the event synchronization function (ESF) (Fig. S5b) gives a more significant correlation for the comparison between Shatuca and Lapa Grande time series (for a −50yr lag) than with the Andean records. Similarly, the ES method shows that several extreme events were synchronous between Shatuca and Lapa Grande throughout the Holocene, while with the other Andean records, the synchronization occurs especially during the late Holocene (Fig. S5c).

5.4. Summer insolation versus oceanic forcing of monsoon rainfall

The decreasing trend seen in the Shatuca $\delta^{18}O$ speleothem record during the Holocene confirms the influence of insolation forcing in a boundary area of the SASM domain, in the mid-altitude Andes. Previous records from the high-altitude Ecuadorian Andes

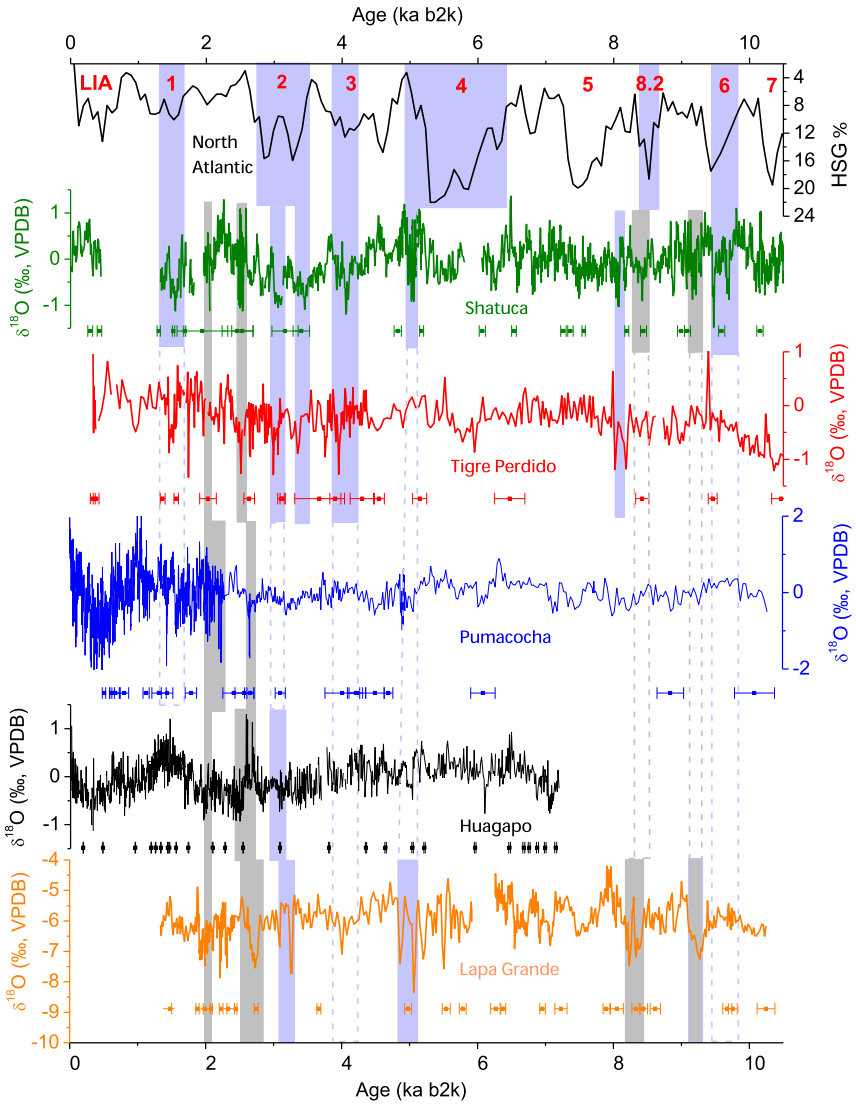

Fig. 4. Comparison between Holocene South American paleo-precipitation records and the North Atlantic Hematite stained grains of Bond et al. (2001). The HSG% record of the North Atlantic Ocean is shown in black, Shatuca cave_detrended record in green (this study), Tigre Perdido cave_detrended record in red (van Breukelen et al., 2008), Pumacocha lake_detrended record in blue (Bird et al., 2011a), Huagapo cave_detrended record in black (Kanner et al., 2013) and Lapa Grande cave in orange (Strikis et al., 2011). Blue bars indicate abrupt changes in Shatuca record which are synchronous with the Bond Events (Event numbers defined in Bond et al., 2001 are marked at the top of the bar). Gray bars represent abrupt changes in Shatuca record probably associated to regional events in South America. Ages and error bar for each record are also shown. (For interpretation of the references to colour in this figure legend, the reader is referred to the web version of this article.)

(Rodbell et al., 1999; Moy et al., 2002) have suggested an increase in the frequency of El Niño events during the late Holocene. Although Andean precipitation in this region is largely influenced by the SASM, the present-day response to El Niño events is very different between the Shatuca and Pallcacocha sites. While rainfall is significantly enhanced at Lake Pallcacocha during extreme El Niño events (Ambrizzi et al., 2004; Garreaud et al., 2009), it causes droughts in the western Amazon and northeastern Andean slopes, where the Shatuca region is located (Espinoza et al., 2011; Lavado and Espinoza, 2014). It is further noteworthy that the changes in lake sedimentation at Pallcacocha, attributed to increased El Niño frequency between 5.0–4.7, 3.5–2.5 and 1.7–1.3 ka b2k (Rodbell et al., 1999; Moy et al., 2002), correspond with periods of more negative $\delta^{18}O$ values in our Shatuca record, indicating enhanced monsoon intensity in the late Holocene in northern Peru (Fig. 5).

Since extreme El Niño events, nowadays, lead to drought in the western Amazon (Espinoza et al., 2011; Lavado and Espinoza, 2014), an increase in El Niño activity during the late Holocene appears inconsistent with the enhanced monsoon rainfall observed during late Holocene in several Andean records at different altitudes (from north to central Peru). The Huagapo cave record (Kanner et al., 2013) in the central Peruvian Andes, however, also recorded dry periods during the last millennia, which the authors attributed to a potential increase in El Niño-like activity, based on a comparison with a Pacific record from off the coast of Peru (Rein et al., 2005), equally suggesting stronger El Niño activity during the late Holocene.

Lake Pallcacocha is exposed to easterly winds that transport moisture from the Amazon basin toward the Andes. Hence, an alternative scenario explaining long-term changes in precipitation at Lake Pallcacocha would involve a progressive intensification of the SASM as austral summer insolation increases over the course of the Holocene, as observed at Shatuca and other Andean records. However, this process might not initially affect distal monsoon areas such as Lake Pallcacocha, where the monsoon influence would only be felt once its intensity increased considerably due to

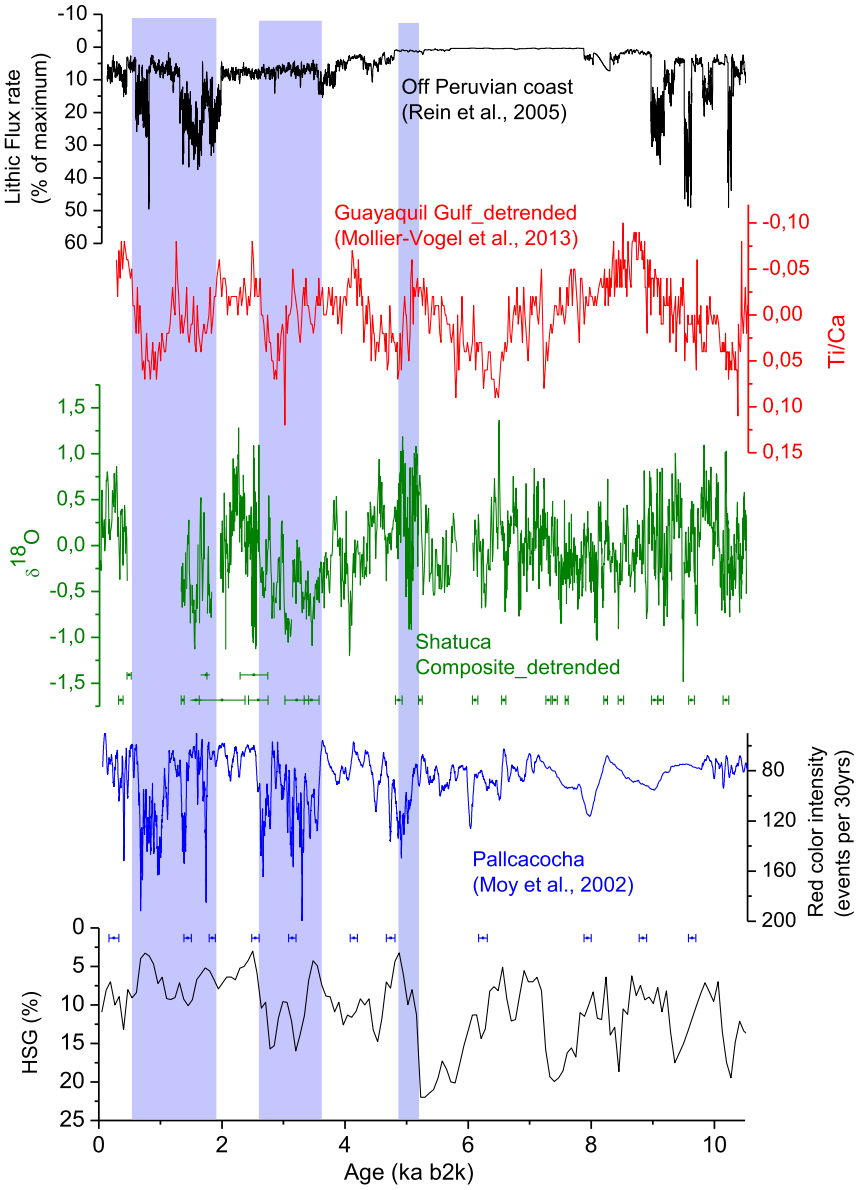

Fig. 5. From top to bottom: Black line: Paleo-ENSO lithic flux reconstruction off the coast of central Peru (Rein et al., 2005). Red line: Guayaquil Gulf sediment detrended record (Mollier-Vogel et al., 2013). Green line: Shatuca $\delta^{18}O$ detrended time-series (this study). Blue line: Pallcacocha lake time series (Moy et al., 2002). Black line: Hematite Stained Grain debris in the North Atlantic (Bond et al., 2001). Blue shading indicates synchronous wet periods in Shatuca cave (this study), Pallcacocha lake (Moy et al., 2002) and the Guayaquil Gulf records (Mollier-Vogel et al., 2013), probably related to Bond events. The 5ka b2k event, occurred in between drier conditions and was characterized in Shatuca record by the most abrupt transitions toward wet conditions of the Holocene. (For interpretation of the references to colour in this figure legend, the reader is referred to the web version of this article.)

higher austral summer insolation starting at 5 ka b2k. In this scenario, the higher erosion rates at Lake Pallcacocha might represent the maximum extent of the monsoon belt in the region reaching the lake, especially during the Bond events. Previous studies have suggested that El Niño events in the Pallcacocha record increased in intensity due to the higher monsoon transport that occurred since the mid Holocene (Haug et al., 2001; Conroy et al., 2008; Toth et al., 2012).

The importance of Atlantic and Amazonian moisture for precipitation over the high summits of the equatorial Andes is confirmed by the Ti/Ca sediment record of Mollier-Vogel et al. (2013) (Fig. 5), from the Gulf of Guayaquil (4°S). This record clearly demonstrates that precipitation over the western Ecuadorian Andes, and hence Ti influx to the marine floor, increased in parallel with austral summer insolation, confirming the influence of the SASM on precipitation variability over the high summits of the Andes.

Although Pallcacocha and Shatuca records show no close resemblance with previous proxy records for ENSO precipitation from the eastern equatorial Pacific during the Holocene (Fig. 5) (Rein et al., 2005; Conroy et al., 2008; Zhang et al., 2014), it is worth considering that an increase in La Niña or La Niña–like events, could have fostered wet events in the eastern Andes if the mean state of ENSO was the same as nowadays. Studies from the eastern Pacific at the Gulf of Panama (Toth et al., 2012) also suggest increased ENSO activity for the last 4 ka b2k. However, they discuss the possibility of alternating El Niño and La Niña states and its coupling with southward ITCZ displacement. Similarly, studies from El Junco lake in the Galapagos Islands (Conroy et al., 2008), suggest increased ENSO variability during the late Holocene period.

In this case, the more frequent El Niño events could have left their record in Lake Pallcacocha while at the same time more frequent La Niña events would have increased precipitation at our Shatuca site.

Our new record from Shatuca cave confirms that the mid-altitude areas in the Andes are quite sensitive to abrupt changes in monsoonal climate, which appear to occur on time scales of a few years to a few decades. Some of these climate anomalies are also apparent in other Andean records from central and northern Peru and in Ecuador, such as the period between 3.5–3.0 ka b2k, which has been identified in Pallcacocha lake and in the Tigre Perdido, Shatuca and Huagapo speleothem records as a period of increased humidity (Figs. 4 and 5) (Moy et al., 2002; van Beukelen et al., 2008; Kanner et al., 2013). These periods of multi-decadal monsoon intensification can be identified in areas with very different El Niño sensitivities, suggesting that they were triggered by changing SST gradients in the tropical Atlantic, rather than by El Niño. This notion is further supported by the correspondence of abrupt monsoon changes with cold episodes in the northern North Atlantic during Bond Events.

6. Conclusions

The Shatuca $\delta^{18}O$ record shows that the northeastern slopes of the Peruvian Andes were exposed to a gradual enhancement of the SASM during the Holocene, reaching its maximum during the late Holocene, in agreement with other isotope records from South America.

Superimposed on this long-term trend, several abrupt changes toward wetter and drier conditions in the Shatuca record appear to be widespread and occurred also at lowland and high-elevation Andean sites in South America.

The temporal correspondence between cold episodes in the North Atlantic during Bond events and some periods of enhanced SASM in the records discussed in this study, reinforce the notion that throughout the Holocene abrupt events in the Andean regions were related to changes in climate conditions in the Atlantic Ocean. The Pacific Ocean may have played a role as well; modulating the SASM activity, but its exact influence remains unclear during the Holocene. The comparison between Shatuca cave and Pallcacocha lake records suggests that long-term maximum increases in SASM precipitation may even have affected the Andes of Ecuador during the late Holocene.

Acknowledgments

This research was undertaken as a part of the PALEOTRACES project (IRD, UPMC, UFF, Uantof, UPCH) and supported by the Brazilian National Council for Scientific and Technological Development – CNPq (grant 158894/2010-3) and the Fundação de Amparo a Pesquisa do Estado de São Paulo-FAPESP through the Dimensions of Biodiversity Program grants #2012/50260-6 and #2013/50297 and PRIMO cooperative project (CNPq – IRD) to F.W. Cruz. MV acknowledges support from NSF (AGS-1303828). We thank Osmar Antunes for this support during the stable isotope data acquisition at São Paulo University. We also thank Augusto Auler, the Groupe Spéléo Bagnols Marcoule (GSBM) and the Espeleo Club Andino (ECA Perú) for the support during the collection of speleothems and for providing us the opportunity to work with them. We are grateful to Jhan Carlo Espinoza, who provided insight and expertise in Peruvian climatology, to Claire Lazareth, Bruno Turcq, Luc Ortlieb, Philip Meyers, J.B. Ponce, C.R. Grijalba and two anonymous reviewers, for their effort and time spent in discussions and comments that greatly improved the manuscript.

Appendix A. Supplementary data

Supplementary data related to this article can be found at http://dx.doi.org/10.1016/j.quascirev.2016.05.023.

References

Abbott, M.B., Binford, M.W., Brenner, M., Kelts, K.R.A., 1997a. 3500 C-14 yr high-resolution record of water-level changes in Lake Titicaca, Bolivia/Peru. Quat. Res. 47, 169–180.

Abbott, M.B., Seltzer, G.O., Kelts, K.R., Southon, J., 1997b. Holocene paleohydrology of the tropical Andes from lake records. Quat. Res. 47, 70–80.

Abbott, M.B., Wolfe, B.B., Wolfe, A., Seltzer, G., Aravena, R., Mark, B.G., Polissar, P.J., Rodbell, D.T., Rowe, H.D., Vuille, M., 2003. Holocene paleohydrology and glacial history of the central Andes using multiproxy lake sediment studies. Palaeogeogr. Palaeoclimatol. Palaeoecol. 194, 123–138.

Ambrizzi, T., de Souza, E.B., Pulwarty, R.S., 2004. The Hadley and Walker regional circulations and associated ENSO impacts on the south American seasonal rainfall. In: Diaz, Henry F., Bradley, Raymond S. (Eds.), The Hadley Circulation: Present, Past and Future, , 1 ed.21. Kluwer Academic Publishers, Netherlands, pp. 203–235.

Apaéstegui, J., Cruz, F.W., Sifeddine, A., Vuille, M., Espinoza, J.C., Guyot, J.L., Khodri, M., Strikis, N., Santos, R.V., Cheng, H., Edwards, L., Carvalho, E., Santini, W., 2014. Hydroclimate variability of the northwestern Amazon basin near the Andean foothills of Peru related to the south American monsoon system during the last 1600 years. Clim. Past 10, 1967–1981. http://dx.doi.org/10.5194/cp-10-1967-2014.

Baker, P.A., Seltzer, G.O., Fritz, S.C., Dunbar, R.B., Grove, M.J., Tapia, P.M., Cross, S.L., Rowe, H.D., Broda, J.P., 2001. The history of South American tropical precipitation for the past 25,000 years. Science 291, 640–643.

Baker, P.A., Fritz, S.C., Garland, J., Ekdahl, E., 2005. Holocene hydrologic variation at Lake Titicaca, Bolivia/Peru, and its relationship to North Atlantic climate variation. J. Quat. Sci. 20, 655–662. http://dx.doi.org/10.1002/jqs.987.

Bigot, J.Y., 2008. La rivière souterraine de Shatuca = El río subterráneo de Shatuca. Bulletin du Groupe Spéléologique Bagnols Marcoule. Hors série spécial Chaquil 2006 & Santiago 2007 52–56.

Bird, B.W., Abbott, M.B., Rodbell, D.T., Vuille, M., 2011a. Holocene tropical South American hydroclimate revealed from a decadally resolved lake sediment $\delta^{18}O$ record. Earth Planet. Sci. Lett. 310, 192–202.

Bird, B.W., Abbott, M.B., Vuille, M., Rodbell, D.T., Stansell, N.D., Rosenmeier, M.F., 2011b. A 2,300-year-long annually resolved record of the South American summer monsoon from the Peruvian Andes. Proc. Natl. Acad. Sci. U. S. A. 108, 8583–8588.

Bond, G., Kromer, B., Beer, J., Muscheler, R., Evans, M.N., Showers, W., Hoffmann, S., Lotti-Bond, R., Hajdas, I., Bonani, G., 2001. Persistent solar influence on North Atlantic climate during the Holocene. Science 294, 2130–2136.

Bookhagen, B., Strecker, M.R., 2008. Orographic barriers, high resolution TRMM rainfall, and relief variations along the eastern Andes. Geophys. Res. Lett. 35, L06403.

Breitenbach, S.F.M., Rehfeld, K., Goswami, B., Baldini, J.U.L., Ridley, H.E., Kennett, D.J., Prufer, K.M., Aquino, V.V., Asmerom, Y., Polyak, V.J., Cheng, H., Kurths, J., Marwan, N., 2012. Constructing proxy records from age models (COPRA). Clim. Past 8, 1765–1779. http://dx.doi.org/10.5194/cp-8-1765-2012.

Buijnzeel, L.A., 2001. Hydrology of tropical montane cloud forests: A reassessment. Land Use and Water Resources Research 1, 1.1–1.18.

Buffen, A.M., Thompson, L.G., Mosley-Thompson, E., Huh, K.I., 2009. Recently exposed vegetation reveals Holocene changes in the extent of the Quelccaya Ice Cap, Peru. Quat. Res. 72, 157.

Bush, M.B., Silman, M.R., Urrego, D.H., 2004. 48,000 Years of climate and forest change in a biodiversity hot spot. Science 303, 827–829.

Bush, M.B., Hansen, B.C.S., Rodbell, D.T., Seltzer, G.O., Young, K.R., Leon, B., Abbott, M.B., Silman, M.R., Gosling, W.D., 2005. A 17 000-year history of Andean climate and vegetation change from Laguna de Chochos, Peru. J. Quat. Sci. 20, 703–714.

Bush, M.B., Hanselman, J.A., Hooghiemstra, H., 2011. Andean Montane forests and climate change. In: Tropical Rainforest Responses to Climatic Change, 2nd. Ed. Springer-Verlag, Berlin Heidelberg, pp. 35–60.

Carlson, A.E., LeGrande, A.N., Oppo, D.W., Came, R.E., Schmidt, G.A., Anslow, F.S., Licciardi, J.M., Obbink, E., 2008. Rapid early Holocene deglaciation of the Laurentide ice sheet. Nat. Geosci. 1, 620–624. http://dx.doi.org/10.1038/ngeo285.

Cheng, H., Fleitmann, D., Edwards, L.R., Wang, X., Cruz, F.W., Auler, A.S., Mangini, A., Wang, Y., Kong, X., Burns, S.J., Matter, A., 2009. Timing and structure of the 8.2 kyr BP event inferred from d18O records of stalagmites from China, Oman, and Brazil. Geology 37, 1007–1010.

Cheng, H., Sinha, A., Wang, X., Cruz, F., Edwards, L., 2012. The global paleomonsoon as seen through speleothem records from Asia and the Americas. Clim. Dyn. 39, 1045–1062. http://dx.doi.org/10.1007/s00382-012-1363-7.

Cheng, H., Sinha, A., Cruz, F.W., Wang, X., Edwards, R.L., d'Horta, F.M., Ribas, C.C., Vuille, M., Stott, L.D., Auler, A.S., 2013a. Climate change patterns in Amazonia and biodiversity. Nat. Commun. 4, 1–6. http://dx.doi.org/10.1038/ncomms2415.

Cheng, H., Edwards, R.L., Shen, C.-C., Polyak, V.J., Asmerom, Y., Woodhead, J., Hellstrom, J., Wang, Y., Kong, X., Spötl, C., Wang, X., Alexander Jr., E.C., 2013b. Improvements in 230Th dating, 230Th and 234U half-life values, and U–Th

isotopic measurements by multi-collector inductively coupled plasma mass spectrometry. Earth Planet. Sci. Lett. 371–372, 82–91.
Claussen, M., 2008. Holocene rapid land cover change – evidence and theory. In: Battarbee, R., Binney, H. (Eds.), Natural Climate Variability and Global Warming. Wiley-Blackwell, Chichester, pp. 232–253.
Cobbing, E.J., Pitcher, W.S., Wilson, J.J., Baldock, J.W., Taylor, W.P., McCourt, W., Snelling, N.J., 1981. The geology of the Western Cordillera of northern Peru. Overseas Mem. Inst. GeolSci. 5, 143.
Conroy, J.L., Overpeck, J.T., Cole, J.E., Shanahan, T.M., Steinitz-Kannan, M., 2008. Holocene changes in eastern tropical Pacific climate inferred from a Galápagos lake sediment record. Quat. Sci. Rev. 27, 1166–1180.
Cordeiro, R.C., Turcq, B., Suguio, K., da Silva, A.O., Sifeddine, A., Volkmer Ribeiro, C., 2008. Holocene fires in East Amazonia (Caraja's), new evidences, chronology and relation with paleoclimate. Glob. Planet. Change 61, 49–62. http://dx.doi.org/10.1016/j.gloplacha.2007.08.005.
Cordeiro, R.C., Turcq, B., Moreira, L.S., Rodrigues, R.A.R., Filho, F.F., Martins, G.S., Santos, A.B., Barbosa, M., da Conceição, M.C.G., Rodrigues, R.C., Evangelista, H., Moreira-Turcq, P., Penido, Y.P., Sifeddine, A., Seoane, J.C.S., 2014. Palaeofires in Amazon: interplay between land use change and palaeoclimatic events. Palaeogeogr. Palaeoclimatol. Palaeoecol. 415, 137–151.
Cruz, F.W., Burns, S.J., Karmann, I., Sharp, W.D., Vuille, M., Cardoso, A.O., Ferrari, J.A., Dias, P.L.S., Viana, O., 2005. Insolation-driven changes in atmospheric circulation over the past 116,000 years in subtropical Brazil. Nature 434, 63–66. http://dx.doi.org/10.1038/Nature03365.
Cruz, F.W., Burns, S.J., Karmannn, I., Sharp, W.D., Vuille, M., 2006. Reconstruction of regional atmospheric circulation features during the late Pleistocene in subtropical Brazil from oxygen isotope composition of speleothems. Earth Planet. Sci. Lett. 248, 494–506.
Dansgaard, W., 1964. Stable isotopes in precipitation. Tellus 16, 436–468. http://dx.doi.org/10.1111/j.2153-3490.1964.tb00181.x.
Espinoza, J.C., Ronchail, J., Guyot, J.L., Junquas, C., Vauchel, P., Lavado, W.S., Drapeau, G., Pombosa, R., 2011. Climate variability and extreme drought in the upper Solimões river (western Amazon basin): understanding the exceptional 2010 drought. Geophys. Res. Lett. 38, L13406. http://dx.doi.org/10.1029/2011GL047862.
EspinozaVillar, J.C., 2009. Impact de la variabilité climatique sur l'hydrologie du bassin amazonien, 207. Université Paris 6-Pierre et Marie Curie, Paris - France. Thèse de Doctorat.
Fleitmann, D., Burns, S.J., Mudelsee, M., Neff, U., Kramers, J., Mangini, A., Matter, A., 2003. Holocene forcing of the indian monsoon recorded in a stalagmite from southern Oman. Science 300, 1737–1739. http://dx.doi.org/10.1126/science.1083130.
Fornace, K.L., Hughen, K.A., Shanahan, T.M., Fritz, S.C., Baker, P.A., Sylva, S.P., 2014. A 60,000-year record of hydrologic variability in the Central Andes from the hydrogen isotopic composition of leaf waxes in Lake Titicaca sediments. Earth Planet. Sci. Lett. 408, 263–271.
Friedman, I., O'Neil, J.R., 1977. Compilation of stable isotope fractionation factors of geochemical interest. In: Data Geochemistry, sixth ed. U.S. Geological Survey Professional. Paper 440, Ch. KK.
Fritsh, F.N., Carlson, R.E., 1980. Monotone piecewise cubic interpolation. SIAM J. Numer. Anal. 238–246.
Garcia, M., Villalba, F., Araguas-Araguas, L., Rozanski, K., 1998. The role of atmospheric circulation patterns in controlling the regional distribution of stable isotope contents in precipitation: preliminary results from two transects in the Ecuadorian Andes. In: Proceedings Series of International Atomic Energy Agency: Isotope Techniques in the Study of Environmental Change, Vienna, IAEA-sm 349/7, pp. 127–140.
Garreaud, R., Vuille, M., Clement, A.C., 2003. The climate of the Altiplano: observed current conditions and mechanisms of past changes. Palaeogeogr. Palaeoclimatol. Palaeoecol. 194, 5–22.
Garreaud, R., Vuille, M., Compagnucci, R., Marengo, J., 2009. Present-day South American climate. Palaeogeogr. Palaeoclimatol. Palaeoecol. 281, 180–195.
Gentry, A.H., 1988. Changes in plant community diversity and floristic composition on environmental and geographical gradients. Ann. Mo. Bot. Gard. 75, 1–34.
Gonfiantini, R., Roche, M.-A., Olivry, J.C., Fontes, J.C., Zuppi, G.M., 2001. The altitude effect on the isotopic composition of tropical rains. Chem. Geol. 181, 147–167.
Grimm, A.M., 2011. Interannual climate variability in South America: impacts on seasonal precipitation, extreme events and possible effects of climate change. Stoch. Environ. Res. Risk Assess. 25, 537–564. http://dx.doi.org/10.1007/s00477-010-0420-1.
Grubb, P.J., 1974. Factors controlling the distribution of forests on tropical mountains: new facts and a new perspective. In: Flenley, J.R. (Ed.), Altitudinal Zonation in Malesia, Geography Department Miscellaneous, Series 16. University of Hull, pp. 1–25.
Grubb, P.J., 1977. Control of forest growth and distribution on wet tropical mountains, with special reference to mineral nutrition. Annu. Rev. Ecol. Syst. 8, 83–107.
Grubb, P.J., Whitmore, T.C.A., 1966. Comparison of montane and lowland rain forest in Ecuador. II. The climate and its effects on the distribution and physiognomy of the forests. J. Ecol. 54, 303–333.
Guyot, J.L., 1993. Hydrogéochimie des fleuves de l'Amazonie bolivienne. Ed. l'ORSTOM.Paris. 261.
Hammer, Ø., Harper, D.A.T., Ryan, P.D., 2001. PAST: Paleontological Statistics Software package for education and data analysis. Palaeontol. Electron. 4, 9.
Hansen, B.C.S., Rodbell, D.T., 1995. A late-glacial/Holocene pollen record from the eastern Andes of northern Peru. Quat. Res. 44, 216–227.
Haug, G.H., Hughen, K.A., Sigman, D.M., Peterson, L.C., Röhl, U., 2001. Southward migration of the intertropical convergence zone through the Holocene. Science 293, 1304–1308.
Hillyer, R., Valencia, B.G., Bush, M.B., Silman, M.R., Steinitz- Kannan, M.A., 2009. 24,700-year paleolimnological history from the Peruvian Andes. Quat. Res. 71, 71–82.
Hurley, J.V., Vuille, M., Hardy, D.R., Burns, S., Thompson, L.G., 2015. Cold air incursions, $\delta^{18}O$ variability and monsoon dynamics associated with snow days at Quelccaya Ice Cap, Peru. J. Geophys. Res. 120, 7467–7487. http://dx.doi.org/10.1002/2015JD023323.
Jarvis, A., Mulligan, M., 2011. The climate of cloud forests. Hydrological Processes 25, 327–343. http://dx.doi.org/10.1002/hyp.7847.
Kanner, L.C., Burns, S.J., Cheng, H., Edwards, R.L., Vuille, M., 2013. High-resolution variability of the South American summer monsoon over the last seven millennia: insights from a speleothem record from the central Peruvian Andes. Quat. Sci. Rev. 75, 1–10. http://dx.doi.org/10.1016/j.quascirev.2013.05.008.
Lachniet, M., 2009. Climatic and environmental controls on speleothem oxygen-isotope values. Quat. Sci. Rev. 28, 412–432.
Laraque, A., Ronchail, J., Cochonneau, G., Pombosa, R., Guyot, J.L., 2007. Heterogeneous distribution of rainfall and discharge regimes in the Ecuadorian Amazon basin. J. Hydrometeorol. 8, 1364–1381.
Laskar, J., Robutel, P., Joutel, F., Gastineau, M., Correia, A.C.M., Levrard, B., 2004. A long-term numerical solution for the insolation quantities of the Earth. Astron. Astrophys. 428, 261–285. http://dx.doi.org/10.1051/0004-6361:20041335.
Lavado, W.L., Espinoza, J.C., 2014. Impactos de El Niño y La Niña en las lluvias del Perú (1965-2007). Rev. Bras. Meteorol. 29, 171–182.
Lavado, W.L., Labat, D., Ronchail, J., Espinoza, J.C., Guyot, J.L., 2012. Trends in rainfall and temperature in the Peruvian Amazon – Andes basin over the last 40 years (1965–2007). Hydrol. Process. 41, 2944–2957. http://dx.doi.org/10.1002/hyp.9418.
León, B., Young, K.R., Brako, L., 1992. Análisis de la composición florística del bosque montano oriental del Perú. In: Young, K.R., Valencia, N. (Eds.), Biogeografía, Ecología y Conservación del Bosque Montano en el Perú, Memorias del Museo de Historia Natural UNMSM, 21, pp. 141–154.
Magny, M., Haas, J.N., 2004. A major widespread climatic change around 5300 cal. yr BP at the time of the Alpine Iceman. J. Quat. Sci. 19, 423–430.
Marengo, J.A., Liebmann, B., Grimm, A.M., Misra, V., Silva Dias, P.L., Cavalcanti, I.F.A., Carvalho, L.M.V., Berbery, E.H., Ambrizzi, T., Vera, C.S., Saulo, A.C., Nogues-Paegle, J., Zipser, E., Sethk, A., Alvese, L.M., 2012. Review: recent developments on the south American monsoon system. Int. J. Climatol. 32, 1–21.
Marengo, J.A., Nobre, C.A., 2001. General Characteristics and Variability of Climate in the Amazon Basin and its Links to the Global Climate System. The Biogeochemistry of the Amazon Basin. Oxford University Press, Oxford, UK, pp. 17–41.
Marengo, J.A., Nobre, C., Tomasella, J., Oyama, M., Sampaio, G., Camargo, H., Alves, L., Oliveira, R., 2008. The drought of Amazonia in 2005. J. Clim. 21, 495–516.
Mayle, F.E., Power, M.J., 2008. Impact of a drier early-mid Holocene climate upon Amazonian forests. Philos. Trans. R. Soc. B 363, 1829–1838.
Mollier-Vogel, E., Leduc, G., Böschen, T., Martinez, P., Schneider, R.R., 2013. Rainfall response to orbital and millennial forcing in northern Peru over the last 18 ka. Quat. Sci. Rev. 76, 29–38.
Moquet, J.-S., Crave, A., Viers, J., Seyler, P., Armijos, E., Bourrel, L., Chavarri, E., Lagane, C., Laraque, A., Lavado Casimiro, W.S., Pombosa, R., Noriega, L., Vera, A., Guyot, J.-L., 2011. Chemical weathering and atmospheric/soil CO2 uptake in the Andean and Foreland Amazon basins. Chem. Geol. 287, 1–26.
Moreira-Turcq, P., Turcq, B., Moreira, L.S., Amorim, M., Cordeiro, R.C., Guyot, J.L., 2014. A 2700 cal yr BP extreme flood event revealed by sediment accumulation in Amazon floodplains. Palaeogeogr. Palaeoclimatol. Palaeoecol. 415, 175–182. http://dx.doi.org/10.1016/j.palaeo.2014.07.037.
Mosblech, N.A.S., Bush, M.B., Gosling, W.D., Hodell, D., Thomas, L., van Calsteren, P., Correa-Metrio, A., Valencia, B.G., Curtis, J., vanWoesik, R., 2012. North Atlantic forcing of Amazonian precipitation during the last ice age. Nat. Geosci. 5, 817–820. http://dx.doi.org/10.1038/NGEO1588.
Moy, C.M., Seltzer, G.O., Rodbell, D.T., Anderson, D.M., 2002. Variability of El Niño/southern oscillation activity at millennial timescales during the Holocene epoch. Nature 420, 162–165.
Nogués-Paegle, J., Mo, K.C., 2002. Linkages between summer rainfall variability over South America and sea surface temperature anomalies. J. Clim. 15, 1389–1407.
Novello, V.F., Cruz, F.W., Karmann, I., Burns, S.J., Stríkis, N.M., Vuille, M., Cheng, H., Edwards, R.L., Barreto, E.A.S., Frigo, E., 2012. Multidecadal climate variability in Brazil's Nordeste during the last 3000 years based on speleothem isotope records. Geophys. Res. Lett. 39, L23706. http://dx.doi.org/10.1029/2012GL053936.
Paegle, J., 1998. A comparative review of South American low-level jets. Meteorologica 3, 73–82.
Poveda, G., Jaramillo, L., Vallejo, L.F., 2014. Seasonal precipitation patterns along pathways of South American low-level jets and aerial rivers. Water Resour. Res. 50, 1–21. http://dx.doi.org/10.1002/2013WR014087.
Quian Quiroga, R., Kreuz, T., Grassberger, P., 2002. Event synchronization: a simple and fast method to measure synchronicity and time delay patterns. Phys. Rev. E 66, 041904. http://dx.doi.org/10.1103/PhysRevE.66.041904.
Rasmussen, S.O., Bigler, M., Blockley, S.P., Blunier, T., Buchardt, S.L., Clausen, H.B., Cvijanovic, I., Dahl-Jensen, D., Johnsen, S.J., Fischer, H., kinis, V., Guillevic, M., Hoek, W.Z., Lowe, J.J., Pedro, J.B., Popp, T., Seierstad, I.K., Steffensen, J.P., Svensson, A.M., Vallelonga, P., Vinther, B.M., Walker, M.J.C., Wheatley, J.J.,

Winstrup, M.A., 2014. Stratigraphic framework for abrupt climatic changes during the Last Glacial period based on three synchronized Greenland ice-core records: refining and extending the INTIMATE event stratigraphy. Quat. Sci. Rev. 106, 14–28.
Rehfeld, K., Kurths, J., 2014. Similarity estimators for irregular and age-uncertain time series. Clim. Past 10, 107–122. http://dx.doi.org/10.5194/cp-10-107-2014.
Rehfeld, K., Marwan, N., Heitzig, J., Kurths, J., 2011. Comparison of correlation analysis techniques for irregularly sampled time series. Nonlinear Process. Geophys. 18, 389–404. http://dx.doi.org/10.5194/npg-18-389-2011.
Rehfeld, K., Marwan, N., Breitenbach, S.F.M., Kurths, J., 2013. Late Holocene Asian Summer Monsoon dynamics from small but complex networks of palaeoclimate data. Clim. Dyn. 41, 3–19. http://dx.doi.org/10.1007/s00382-012-1448-3.
Rein, B., Lückge, A., Reinhardt, L., Sirocko, F., Wolf, A., Dullo, W.-C., 2005. El Niño variability off Peru during the last 20,000 years. Paleoceanography 20, PA4003.
Reuter, J., Stott, L., Khider, D., Sinha, A., Cheng, H., Edwards, R.L., 2009. A new perspective on the hydroclimate variability in northern South America during the Little Ice Age. Geophys. Res. Lett. 36, L21706. http://dx.doi.org/10.1029/2009GL041051.
Rodbell, D.T., Seltzer, G.O., Anderson, D.M., Abbott, M.B., Enfield, D.B., Newman, J.H., 1999. A 15,000-year record of El-Niño alluviation in southwestern Ecuador. Science 283, 516–520.
Ronchail, J., Gallaire, R., 2006. ENSO and rainfall along the Zongo valley (Bolivia) from the Altiplano to the Amazon basin. Int. J. Climatol. 26, 1223–1236.
Salati, E., Dall'Olio, A., Matsui, E., Gat, J.R., 1979. Recycling of water in the Amazon basin - isotopic study. Water Resour. Res. 15, 1250–1258.
Schmidt, G., Le Grande, A., Hoffmann, G., 2007. Water isotope expressions of intrinsic and forced variability in a coupled ocean-atmosphere model. J. Geophys. Res. 112, D10103.
Seltzer, G., Rodbell, D., Burns, S., 2000. Isotopic evidence for late Quaternary climatic change in tropical South America. Geology 28, 35–38.
Shulz, M., Mudelsee, M., 2002. REDFIT: estimating red-noise spectra directly from unevenly spaced paleoclimatic time series. Comput. Geosci. 28, 421–426.
Stansell, N.D., Rodbell, D.T., Abbott, M.B., Mark, B.G., 2013. Proglacial lake sediment records of Holocene climate change in the western Cordillera of Peru. Quat. Sci. Rev. 70, 1–14.
Strikis, N.M., Cruz Jr., F.W., Cheng, H., Karmann, I., Edwards, R.L., Vuille, M., Wang, X., de Paula, M.S., Novello, V.F., Auler, A.S., 2011. Abrupt variations in South American monsoon rainfall during the Holocene based on a speleothem record from central-eastern Brazil. Geology 39, 1075–1078.
Thompson, L.G., Mosley-Thompson, E., Brecher, H., Davis, M., León, B., Les, D., Lin, P., Mashiotta, T., Mountain, K., 2006. Abrupt tropical climate change: Past and present. Proceedings of the National Academy of Science 103, 10536–10543. http://dx.doi.org/10.1073_pnas.0603900103.
Torrence, C., Compo, G.P., 1998. A practical guide to wavelet analysis. Bull. Am. Meteorol. Soc. 79, 61–78.
Toth, L.T., Aronson, R.B., Vollmer, S.V., Hobbs, J.W., Urrego, D.H., Cheng, H., Enochs, I.C., Combosch, D.J., van Woesik, R., Macintyre, I.G., 2012. Enso drove 2500-Year collapse of eastern pacific coral reefs. Science 37, 81–84. http://dx.doi.org/10.1126/science.1221168.
Urrego, D.H., Bush, M.B., Silman, M.R., 2010. A long history of cloud and forest migration from Lake Consuelo, Peru. Quat. Res. 73, 364–373.
Valencia, B.G., Urrego, D.H., Silman, M.R., Bush, M.B., 2010. From ice age to modern: a record of landscape change in an Andean cloud forest. J. Biogeogr. 37, 1637–1647.
van Breukelen, M.R., Vonhof, H.B., Hellstrom, J.C., Wester, W.C.G., Kroon, D., 2008. Fossil dripwater in stalagmites reveals Holocene temperature and rainfall variation in Amazonia. Earth Planet. Sci. Lett. 275, 54–60.
Vimeux, F., Gallaire, R., Bony, S., Hoffmann, G., Chiang, J.C.H., 2005. What are the climate controls on dD in precipitation in the Zongo Valley (Bolivia)? Implications for the Illimani ice core interpretation. Earth Planet. Sci. Lett. 240, 205–220.
Vuille, M., Werner, M., 2005. Stable isotopes in precipitation recording South American summer monsoon and ENSO variability - observations and model results. Clim. Dyn. 25, 401–413.
Vuille, M., Bradley, R.S., Keimig, F., 2000. Climatic variability in the Andes of Ecuador and its relation to tropical Pacific and Atlantic sea surface temperature anomalies. J. Clim. 13, 2520–2535.
Vuille, M., Bradley, R.S., Werner, M., Healy, R., Keimig, F., 2003. Modeling $\delta^{18}O$ in precipitation over the tropical Americas: 1. Interannual variability and climatic controls. J. Geophys. Res. 08, 4174–4175. http://dx.doi.org/10.1029/2001JD002039.
Vuille, M., Burns, S.J., Taylor, B.L., Cruz, F.W., Bird, B.W., Abbott, M.B., Kanner, L.C., Cheng, H., Novello, V.F., 2012. A review of the South American monsoon history as recorded in stable isotopic proxies over the past two millennia. Clim. Past 8, 1309–1321. http://dx.doi.org/10.5194/cp-8-1309-2012.
Walker, J.C., Berkelhammer, M., Bjorck, S., Cwynar, L.C., Fisher, D.A., Long, A.J., Lowe, J.J., Newnham, R.M., Rasmussen, S.O., Weiss, H., 2012. Formal subdivision of the Holocene series/epoch: a discussion paper by a working group of INTIMATE (integration of ice-core, marine and terrestrial records) and the subcommission on Quaternary stratigraphy (international commission on stratigraphy). J. Quat. Sci. 27, 649–659. http://dx.doi.org/10.1002/jqs.2565.
Wang, X., Auler, A.S., Edwards, R.L., Cheng, H., Ito, E., Solheid, M., 2006. Interhemispheric anti-phasing of rainfall during the last glacial period. Quat. Sci. Rev. 25, 3391–3403.
Webster, G.L., 1995. The panorama of Neotropical cloud forests. In: Churchill, S.P., Balslev, H., Forero, E., Luteyn, J.L. (Eds.), Biodiversity and Conservation of Neotropical Montane Forests. New York Botanical Garden, Bronx, pp. 53–77.
Young K.R. and León B. Peru's humid eastern montane forests: an overview of their physical settings, biological diversity, human use and settlement, and conservation needs. DIVA, Technical Report n°5.
Young, K.R., 1991. Floristic diversity on the eastern slopes of the Peruvian Andes. Candollea 46, 125–143.
Young, K.R., 1992. Biogeography of the montane forest zone of the eastern slopes of Peru. In: Young, K.R., Valencia, N. (Eds.), Biogeografía, Ecología y Conservación del Bosque Montano en el Perú. Memorias del Museo de Historia Natural, 21. U.N.M.S.M, Lima, pp. 119–140.
Zhang, Z., Leduc, G., Sachs, J., 2014. El Niño evolution during the Holocene revealed by a biomarker rain gauge in the Galápagos Islands. Earth Planet. Sci. Lett. 404, 420–434.